No. 132/24, 20–34
ISSN 2657-6988 (online)
ISSN 2657-5841 (printed)
DOI: 10.26408/132.02

Submitted: 14.05.2024
Accepted: 02.07.2024
Published: 18.12.2024

EFFECT OF MAINS COMMUNICATION VOLTAGE ON INDUCTION MOTORS

Piotr Gnaciński[1], Damian Hallmann[2]*

[1, 2] Gdynia Maritime University, Morska 81–87, 81–225 Gdynia, Poland, Faculty of Electrical Engineering, Department of Marine Electrical Power Engineering

[1] ORCID 0000-0003-3903-0453, email: p.gnacinski@we.umg.edu.pl

[2] ORCID 0000-0003-4129-8336, email: d.hallmann@we.umg.edu.pl

*Corresponding author

Abstract: Power system lines are not only used for electric energy transfer, but also for the transmission of a communication signal, called the mains communication voltage. The mains communication voltage is in the form of a telegram code, superimposed on the fundamental voltage harmonic. From the point of view of power quality, mains communication voltage should be considered as interharmonics – components of frequency being not equal to the integer multiple of the fundamental frequency. Interharmonics have a negative impact on various energy receivers, including rotating machinery. This study is devoted to the effect of the mains communication voltage on an induction motor. The results of numerical computations on currents and electromagnetic torque pulsations are presented for a four-pole cage induction motor of rated power 3 kW.

Keywords: interharmonics, power quality, cage induction motor, mains communication voltage, ripple control, voltage waveform distortions.

1. INTRODUCTION

Power lines are used not only to transmit electricity, but also to transmit communication signals [Bollen and Gu 2006; Yang and Dennetière 2009; Dzung, Berganza and Sendin 2011; Battacharyya, Cobben and Toonen 2013; Garma and Šesnić 2014; Rahman et al. 2019; Boutsiadis, Tsiamitros and Stimoniaris 2021; 2022; Tsiakalos et al. 2021; Muttaqi et al. 2022], called the '*mains communication voltage*' (MCV) [EN 50160 2010/A2:2019]. It is a solution used in Australia, Austria, Belgium, Bosnia and Herzegovina, Croatia, Montenegro, the Czech Republic, Finland, France, Germany, Greece, Hungary, Ireland, Japan, Libya, Luxembourg, Macedonia, the Netherlands, New Zealand, South Africa, Serbia, Slovenia, Slovakia and the USA, among others [Garma and Šesnić 2014]. The permitted frequencies and values of the mains communication signal are defined in EN 50160, *Voltage characteristics of electricity supplied by public electricity*

networks [EN 50160 2010/A2:2019]. According to EN 50160 2010/A2: 2019, the mains communication signal frequency should be between 0.1 kHz and 100 kHz, and the permitted signal value depends on the frequency. For the 0.1 kHz to 0.4 kHz frequency range, "for 99% of a day the 3 s mean value of signal voltages shall be less or equal to 9%" [EN 50160 2010/A2:2019]. In practice, such a provision allows the use of MCVs of arbitrarily large values, provided that the total duration of the mains communication signal does not exceed 14 minutes and 24 seconds a day [Gnaciński et al. 2023]. Also note EN 50160 2010/A2:2019 specifies that for frequencies higher than 0.4 kHz, the permissible value of the mains communication signal is lower. For 0.4 kHz to 1 kHz frequencies, the signal value gradually decreases to 5%, for 1 kHz to 10 kHz frequencies, the signal value is constantly 5%, and for 1 kHz to 100 kHz, the signal value gradually decreases to 1%.

The MCV is in the form of a telegram code [Rahman et al. 2019; 2022] with a duration of, for example, ~100 s [Yang and Dennetière 2009], generated by static converters in medium-voltage systems [Yang and Dennetière 2009; Dzung, Berganza and Sendin 2011; Rahman et al. 2019]. The typical value of the MCV generated is 1 to 5% of the rated system voltage [Garma and Šesnić 2014]; nevertheless, resonant phenomena in the system can increase this voltage [Yang and Dennetière 2009]. The MCV passes from the medium-voltage system, via transformers, to the low-voltage side [Yang and Dennetière 2009; Dzung, Berganza and Sendin 2011; Rahman et al. 2019], where it is used to control various electrical equipment. For example, the MCV of the system is used to control photovoltaic systems (to prevent overproduction of electrical power), electricity meters, street lights, or to temporarily switch off certain loads during peak energy times, like heat pumps, water heaters, swimming pool pumps, etc. [Dzung, Berganza, and Sendin 2011; Tsiakalos et al. 2021]. Specific loads can understand an individual MCV code [Dzung, Berganza and Sendin 2011]. Note that the control of, for example, PV systems using the MCV of the system or grid is cheaper than commanding these PV systems with data over the Internet and, in addition, is cyber-secure [Boutsiadis, Tsiamitros and Stimoniaris 2021; 2022].

Considering electrical power quality, the MCV of the system should be considered as an instance of voltage interharmonics – that is, components with frequencies that are not an integer multiple of the fundamental harmonic frequency. Note that there are many sources of interharmonics in electrical power systems. They are generated by time-varying power loads, power electronic devices like inverters, renewable energy sources like wind turbines and PV arrays, [Testa et al. 2007; Arkkio et al. 2018; Nassif 2019; Ravindran et al. 2020; Avdeev et al. 2021], among others. Cyclic voltage fluctuations can be considered as a composite of the fundamental voltage harmonic and components with frequencies lower than the fundamental harmonic frequency, meaning interharmonics and subharmonics [Gallo et al. 2005; Bollen and Gu 2006; Tennakoon, Perera and Robinson 2008; Ghaseminezhad et al. 2021b; Gnaciński et al. 2022].

Voltage interharmonics interfere with the operation of a variety of electrical equipment types, like light sources, transformers, control systems, power electronic devices and electrical machines [Gallo et al. 2005; Tennakoon, Perera and Robinson 2008; Ghaseminezhad et al. 2017; 2018; Gnaciński et al. 2019b; Ghaseminezhad et al. January 2021a,b; Gnaciński et al. 2021; 2022; 2023], which are considered particularly sensitive to interharmonic effects. Interharmonics can result in excessive vibration and torsional oscillations, increased power losses, as well as torque and speed fluctuations, among other effects. A similar effect is caused by a mains communication voltage which interferes with the operation of light sources, audio devices, devices which count voltage transitions through zero and induction motors, among others [Battacharyya, Cobben and Toonen 2013; Rahman et al. 2019; Muttaqi et al. 2022; Gnaciński et al. 2023]. Earlier work by the authors [Gnaciński et al. 2023] showed that MCV can cause torque fluctuations of 50% of the rated torque and vibrations in an induction motor, resulting in damage to the machine (the vibration damage evaluation zone D according to ISO 10816-1 1995; ISO 20816-1 2016).

To the authors' knowledge, Gnaciński et al. 2023 is the only paper published which deals with the effect of MCV on an induction motor. Note that the main objective of Gnaciński et al. 2023 was to demonstrate that the permissible voltage limits specified in EN 50160 2010/A2:2019 are too tolerant and fail to protect induction motors from damage. In practice, [Gnaciński et al. 2023] do not exhaust the issue of the MCV effects on induction motors, a problem which needs further development. The research in [Gnaciński et al. 2023] should lead to the formulation of a proposal to modify EN 50160 2010/A2:2019 and establish new MCV limits. In practice, the formulation of a proposal for modification of EN 50160 2010/A2:2019 requires an in-depth investigation into the MCV effects of the system on various electrical loads and, in particular, on electrical machinery.

One issue that needs to be developed further is the effect of the moment of inertia of a driven unit on the detrimental phenomena emerging in an induction motor in response to the MCV of the power system. As demonstrated in [Gnaciński et al. 2019a; 2021; 2022], the moment of inertia of the driven unit has a significant effect on the current levels and torque variations of an induction motor supplied with a voltage which features subharmonics and interharmonics. What needs to be stressed here is that the most damaging phenomena occurring in an induction motor supplied with a voltage which features subharmonics and interharmonics – namely vibration and torsional oscillation – are directly caused by torque fluctuations [Gnaciński et al. 2019b; 2021; 2022; 2023].

At the same time, the investigation into the effects of MCV of the power system on torque fluctuations was limited in Gnaciński et al. 2023 to a case in which the moment of inertia of the driven unit was significantly smaller than the moment of inertia of the driving motor.

The objectives of this paper are formulated considering the problems highlighted above. The main objective is to complement the research results presented in Gnaciński et al. 2023 and to assess the effect of the moment of inertia of the driven unit on the detrimental phenomena in the induction motor caused by the MCV of the power system. The current levels and torque of the motor were studied in this work using a finite element method (FEM). The results of the calculations are presented for a four-pole squirrel-cage induction motor rated at a power of 3 kW.

2. MOTOR MODEL

The test object was a squirrel-cage induction motor, type TSg 100L-4B type, with selected parameters listed in Table 1. A two-dimensional motor model was implemented in the ANSYS Electronics Desktop 2022R2.4 environment (previously known as ANSYS Maxwell). The temperature of the stator and rotor windings was determined using a thermal equivalent motor diagram. The effects of vibration and deformation were disregarded.

Table 1. Selected parameters of the test motor type TSg 100L-4B

Specification	Value
Nominal power [kW]	3
Rated voltage [V]	380
Rated current [A]	6.9
Rated power factor [-]	0.81
Rated speed [rpm]	1420
Moment of inertia [kg m^2]	0.00702299
Winding connection system	Delta

The initial subdivision mesh was generated using the RMxprt module and then condensed from a convergence analysis performed on the calculation results. The tau subdivision mesh used contained approximately 22,000 elements. The maximum edge length of the finite elements was about 2.5 mm in the rotor core and about 4.9 mm in the stator core. To improve the convergence of the solution, areas with a condensed subdivision mesh, such as the air gap, were introduced. The subdivision mesh is shown in Figure 1.

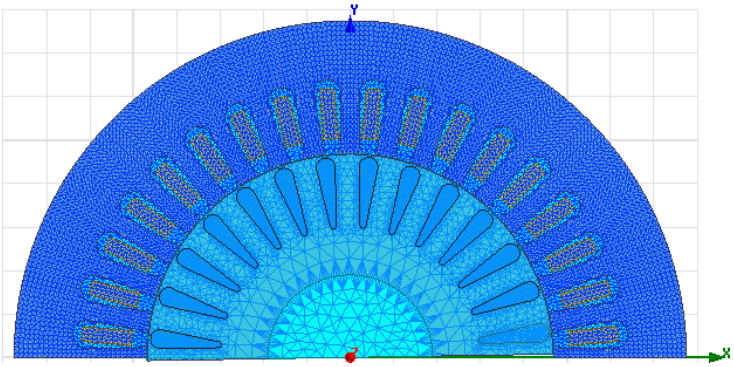

Fig. 1. Mesh used

Source: own study.

The parameters of the model were identified based on the engine structural data and experimental results. The interharmonics present in the voltage were modelled using an external power supply circuit generated in Maxwell Circuit Editor. The external power circuit comprised electromotive forces connected in series to modulate the fundamental voltage harmonic and the interharmonic in each phase (Fig. 2). Calculations were performed using a transient solver.

The model was verified experimentally in earlier work by the authors, e.g. [Gnaciński et al. 2019a; 2021]. For a more detailed description of the model, see [Gnaciński et al. 2019a; 2021].

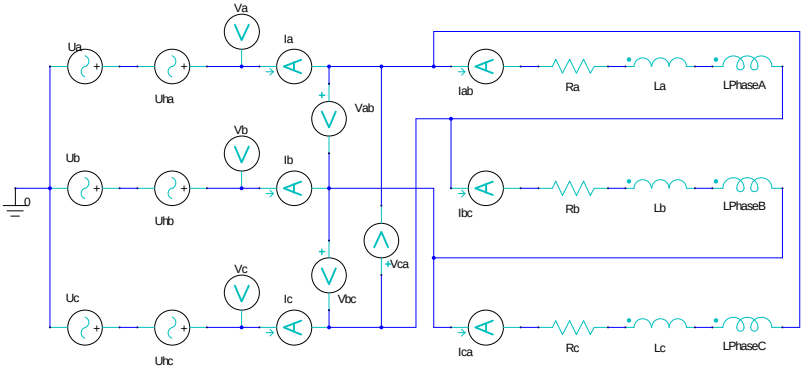

Fig. 2. Example of an external power supply circuit generated in Maxwell Circuit Editor; U_a, U_b, U_c — voltage sources modelling the fundamental harmonic of the supply voltage; U_{ha}, U_{hb}, U_{hc} – voltage sources modelling the interharmonic; R_a, R_b, R_c – resistance levels of individual winding bands; L_a, L_b, L_c – 9.45 mH; L_{PhaseA}, L_{PhaseB}, L_{PhaseC} – 94.1 mH – inductance levels of the winding ends and the grooved section of the stator windings

Source: own study.

3. RESULTS

Below are the calculation results for the motor's supply current and torque. The results are presented for two extreme cases – a negligible moment of inertia (NMI) load operation and constant rotational speed (CRS) operation, which roughly corresponded to loaded operation with a moment of inertia significantly greater than the motor's moment of inertia. For simplicity, it was assumed that a single interharmonic of the positive sequence and a value equal to 9% of the rated voltage is present in the supply voltage. In addition, the motor load torque was assumed to be negligible, making the presented calculation results fully comparable with those in [Gnaciński et al. 2023] (limited to NMI). Note that the highest oscillations of an induction motor supplied with a voltage with subharmonics and interharmonics occur at idle speed, and that induction motors driving some equipment [Singh and Chelliah 2017; Singh et al. 2020] can temporarily operate at a load much lower than the rated load.

Figures 3 and 4 show the current waveforms for a voltage interharmonic with f_{ih} = 101 Hz with CRS and NMI, respectively. The spectra of the waveforms are shown in Fig. 5 and 6. For CRS (Fig. 5), the fundamental harmonic current was 65.14% of the rated current (I_{nom}) and the interharmonic current at f_{ih} = 101 Hz is 29.74% I_{nom}. For NMI (Fig. 6), the fundamental current harmonic and interharmonic were equal to 65.70% I_{nom} and 36.74% I_{nom}. The differences were due to variations in speed for the NMI case. As demonstrated by [Gnaciński et al. 2019a,b; 2021; 2022], rpm fluctuations can significantly amplify the detrimental phenomena occurring in an induction motor supplied with a voltage which features subharmonics and interharmonics. The rpm fluctuations are caused by torque pulsations, the frequency of which could be determined using a relationship [Tennakoon, Perera and Robinson 2008]:

$$f_p = f_{ih} - f_1 \tag{1}$$

with:

f_p – torque pulsation frequency for a supply voltage with a positive sequence interharmonic;
f_{ih} – interharmonic frequency;
f_1 – fundamental harmonic frequency of the supply voltage.

Note that for subharmonics and interharmonics with frequencies below 100 Hz, the differences between CRS and NMI were much larger [Gnaciński et al. 2019a; 2021]. In addition, the current spectra shown in Figures 5 and 6 did not contain subharmonic components. Their presence was detected for supply voltages featuring interharmonics that were below 100 Hz [Gnaciński et al. 2021].

The next graph (Fig. 7) compares the characteristics of the current interharmonics vs. the voltage interharmonic frequency, f_{ih} for CRS and NMI. The relevant characteristics for NMI were adopted from [Gnaciński et al. 2023]. Figure 7 demonstrates that, for the motor of interest, the moment of inertia of the driven unit had relatively little effect on the flow of current interharmonics. The effect was virtually negligible for interharmonics with frequencies above approx. 150 to 200 Hz. In comparison, the effect of the moment of inertia of the driven unit on current interharmonics was significant for voltage interharmonics that were below 100 Hz [Gnaciński et al. 2021].

As already mentioned, vibration and torsional oscillations of rotating machinery should be considered as particularly harmful phenomena caused by subharmonics and interharmonics. Their direct cause is torque pulsations [Gnaciński et al. 2019b; 2021; 2022; 2023].

Figures 8 and 9 show the motor torque waveforms for CRS, NMI and an interharmonic at f_{ih} = 101 Hz. The spectra of the waveforms are shown in Figures 10 and 11. In both charts, the highest torque component had a frequency of 51 Hz, defined by the relation (1). The other frequency components were much smaller. The component was equal to 38.78% of the rated torque (T_{nom}) for CRS (Fig. 8) and 50.24% T_{nom} for NMI (Fig. 9). For comparison, for the tested motor supplied with a voltage featuring an interharmonic at f_{ih} = 80 Hz, the torque component at the frequency determined by relation (1) was about four times higher for NMI than for CRS [Gnaciński et al. 2021].

Figure 12 shows the characteristics of the considered torque pulse component as a function of the voltage interharmonic frequency, f_{ih} for CRS and NMI. For the NMI, the characteristics were quoted from Gnaciński et al. 2023. As in the case of current interharmonics, the moment of inertia of the driven unit had virtually no effect on the motor torque pulsations with interharmonics at frequencies above approximately 200 Hz.

In summary, for the interharmonic frequency range considered, the effect of the driven unit's moment of inertia on the motor current levels and torque pulsations was relatively small and much lower than for interharmonic frequencies below 100 Hz [Gnaciński et al. 2021]. This was probably due to the high frequency of torque pulsations (50 to 350 Hz). Consequently, speed fluctuations were strongly damped by the motor's moment of inertia. Moreover, for the interharmonic frequency range of interest, there was no rigid-body torsional resonance observed for subharmonics and interharmonics less than 100 Hz [Ghaseminezhad et al. 2018; 2021b; Gnaciński et al. 2019b; 2021; 2022].

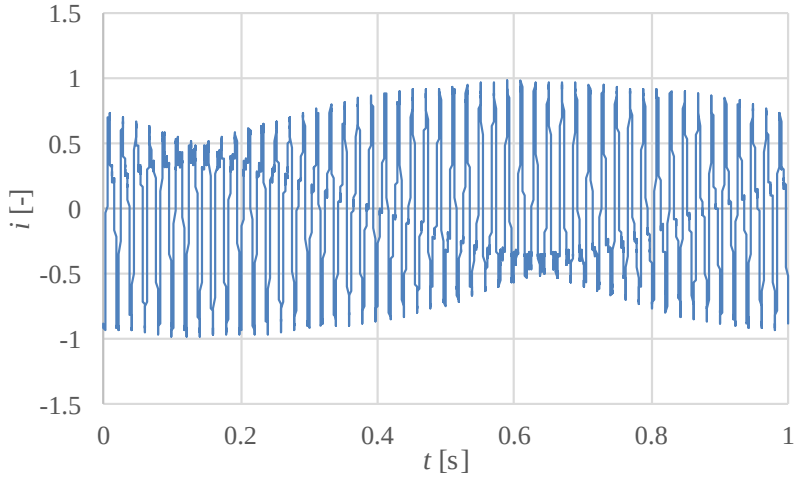

Fig. 3. Motor current draw waveform for CRS and f_{ih} = 101 Hz interharmonic motor voltage

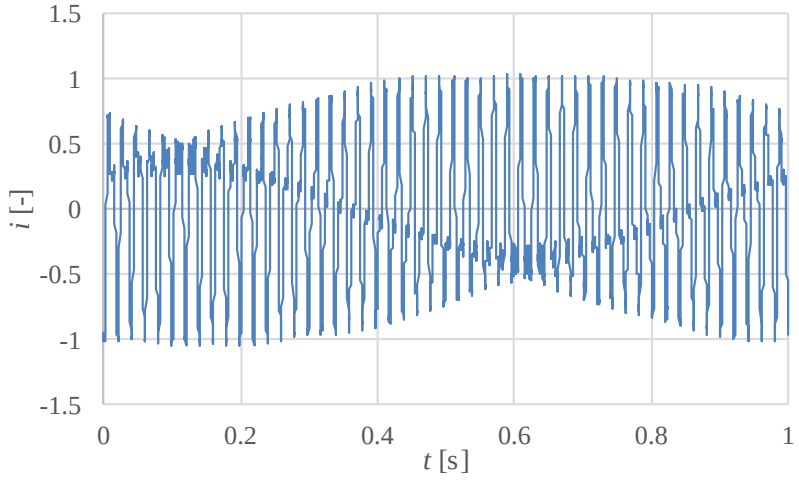

Fig. 4. Motor current draw waveform for NMI and f_{ih} = 101 Hz interharmonic motor voltage

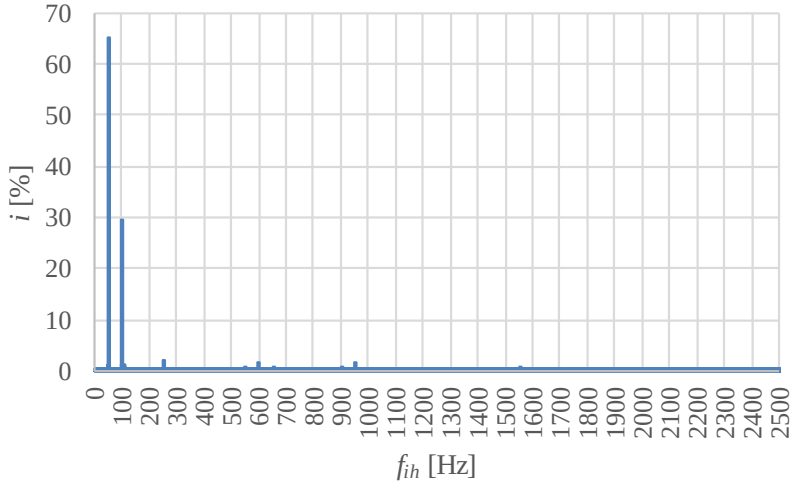

Fig. 5. Motor current draw spectrum for CRS and f_{ih} = 101 Hz interharmonic motor voltage; the frequency components were referenced to the rated current

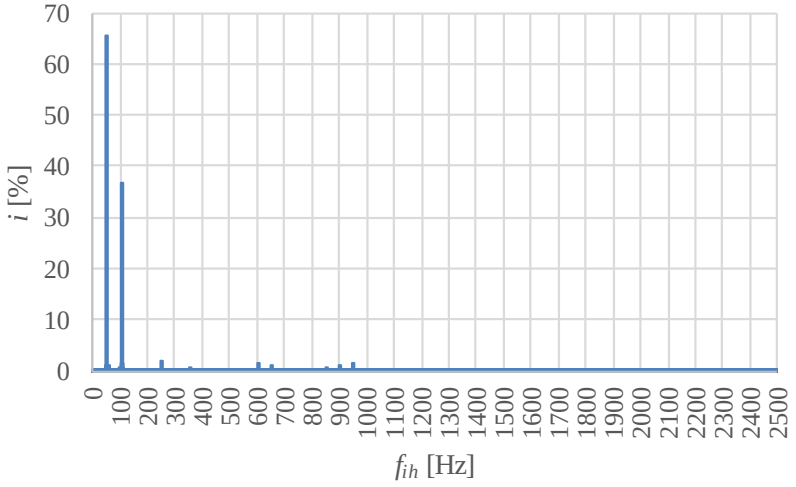

Fig. 6. Motor current draw spectrum for NMI and f_{ih} = 101 Hz interharmonic motor voltage; the frequency components were referenced to the rated current

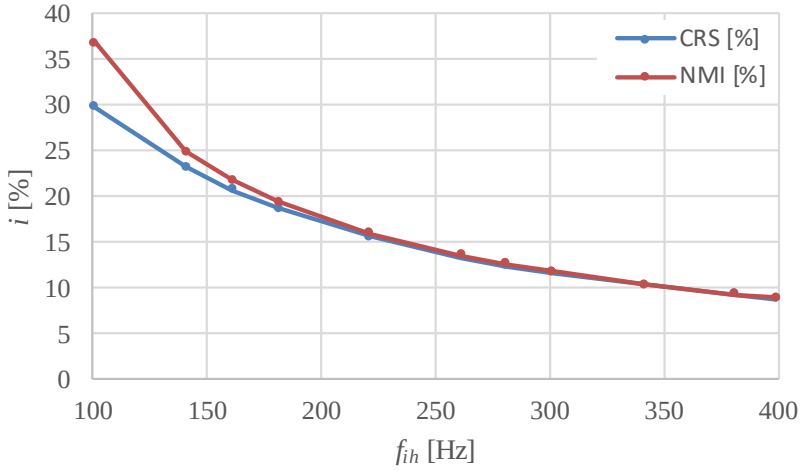

Fig. 7. Characteristics of the current interharmonics vs. interharmonic frequency for CRS and NMI; the frequency components were referenced to the rated current

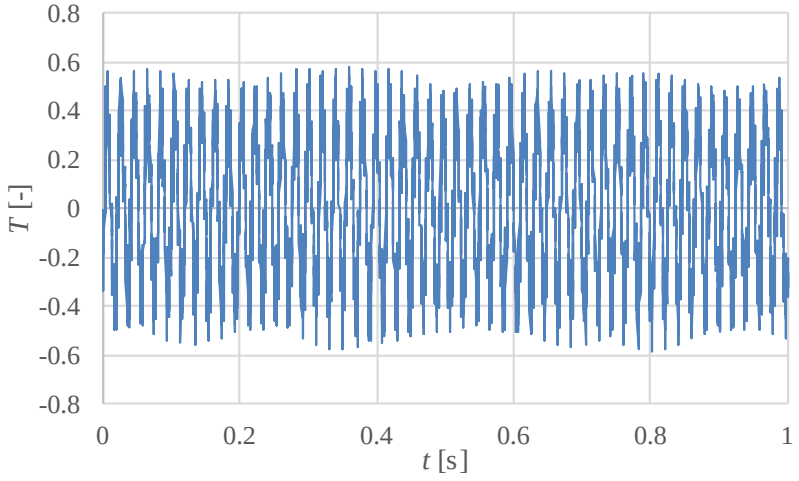

Fig. 8. Torque waveform (reference: rated torque) for CRS and f_{ih} = 101 Hz interharmonic voltage

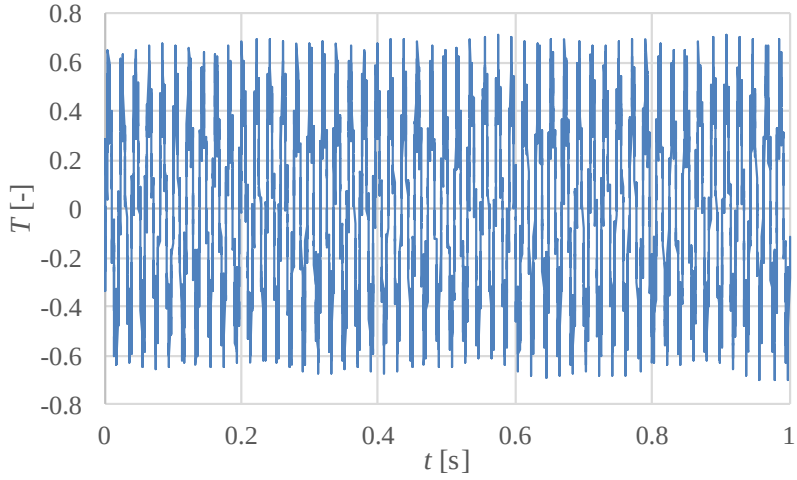

Fig. 9. Torque waveform (reference: rated torque) for NMI and f_{ih} = 101 Hz interharmonic voltage

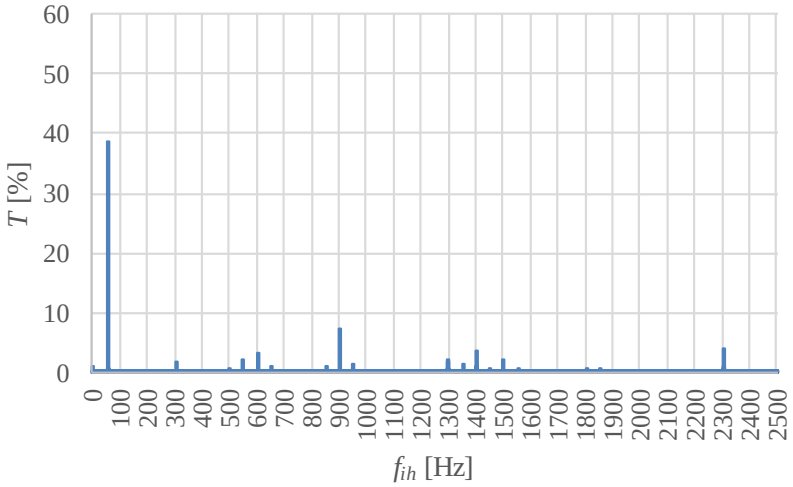

Fig. 10. Motor torque spectrum for CRS and f_{ih} = 101 Hz interharmonic motor voltage; the frequency components were referenced to the rated torque

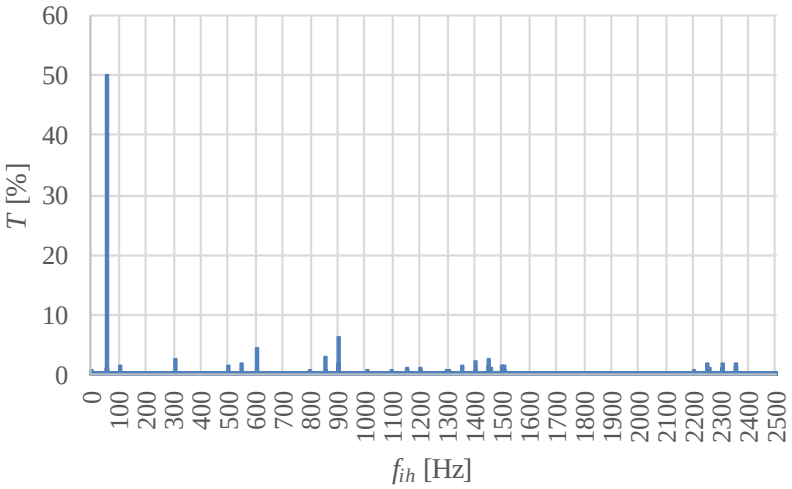

Fig. 11. Motor torque spectrum for NMI and f_{ih} = 101 Hz interharmonic motor voltage; the frequency components were referenced to the rated torque

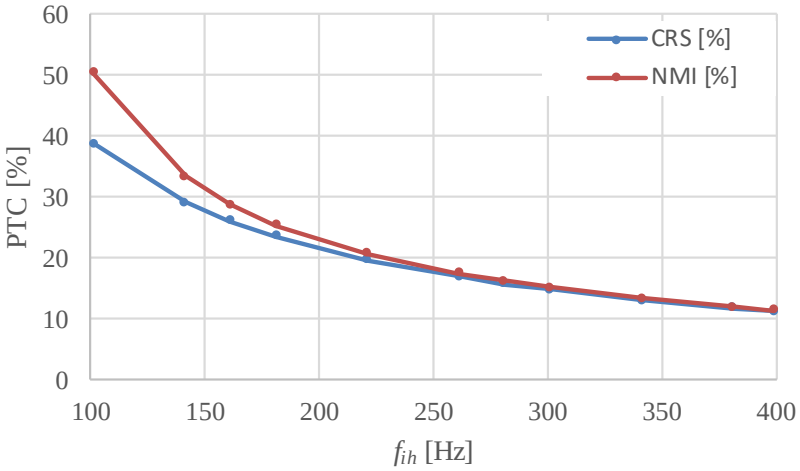

Fig. 12. Characteristics of the torque pulse component at the frequency determined with (1) vs. voltage interharmonic frequency for CRS and NMI; the frequency components were referenced to the motor rated torque

4. CONCLUSIONS

Previous investigations into the effect of the mains communication voltage (MCV) on induction motors [Gnaciński et al. 2023] were carried out ignoring the effect of the moment of inertia of driven units coupled to such motors. However, as demonstrated by [Gnaciński et al. 2019b; 2021; 2022], the detrimental phenomena occurring in an induction motor supplied with a voltage that features subharmonics and interharmonics (like current subharmonic and interharmonic flows and torque pulsations) significantly depend on the moment of inertia of the driven unit. The results presented in this paper demonstrate that, for the interharmonic frequency range corresponding to the MCV, the moment of inertia of the driven unit has a relatively small effect (at voltage interharmonic frequencies of less than about 150 Hz to 200 Hz in the case of the tested motor) or even an negligible effect (for voltage interharmonic frequencies greater than about 150 Hz to 200 Hz) on the current interharmonics and torque pulsations of the motor. This is probably due to the strong damping of speed fluctuations by the motor's moment of inertia for the interharmonic frequency range considered. Moreover, there is no rigid-body torsional vibration resonance for the range of interest.

REFERENCES

Arkkio, A., Cederström, S., Awan, H.A.A., Saarakkala, S.E., Holopainen, T.P., 2018, *Additional Losses of Electrical Machines Under Torsional Vibration*, IEEE Transactions on Energy Conversion, vol. 33, pp. 245–251.

Avdeev, B.A., Vyngra, A.V., Chernyi, S.G., Zhilenkov, A.A., Sokolov, S.S., 2021, *Evaluation and Procedure for Estimation of Interharmonics on the Example of Non-Sinusoidal Current of an Induction Motor with Variable Periodic Load*, IEEE Access, vol. 9, pp. 158 412–158 419.

Battacharyya, S., Cobben, S., Toonen, J., 2013, *Impacts of Ripple Control Signals at Low Voltage Customer's Installations*, 22nd International Conference on Electricity Distribution, Stockholm, Sweden, 10–13 June.

Bollen, M.H.J., Gu, I.Y.H., 2006, *Origin of Power Quality Variations. Signal Processing of Power Quality Disturbances*, Wiley, New York, USA, pp. 41–162.

Boutsiadis, E., Tsiamitros, D., Stimoniaris, D., 2021, *Distributed Generation Control Via Ripple Signaling for Establishment of Ancillary Services in Distribution Networks*, 13th International Conference on Electrical and Electronics Engineering (ELECO), Bursa, Turkey, November, pp. 18–23.

Boutsiadis, E., Tsiamitros, D., Stimoniaris, D., 2022, *Ripple Signaling Control for Ancillary Services in Distribution Networks*, Turkish Journal of Electrical Power Energy Systems, vol. 2(1), pp. 31–45.

Dzung, D., Berganza, I., Sendin, A., 2011, *Evolution of Powerline Communications for Smart Distribution: From Ripple Control to OFDM*, IEEE International Symposium on Power Line Communications and Its Applications, Udine, Italy, April, pp. 474–478.

EN 50160, 2010/A2:2019, *Voltage Characteristics of Electricity Supplied by Public Electricity Networks*.

Gallo, D., Landi, C., Langella, R.A., Testa, A., 2005, *Limits for Low Frequency Interharmonic Voltages: Can They Be Based on the Flickermeter Use*, IEEE Russia Power Tech, St. Petersburg, Russia, June, pp. 1–7.

Garma, T., Šesnić, S., 2014, *Measurement and Modeling of the Propagation of the Ripple Control Signal through the Distribution Network*, International Journal of Electrical Power & Energy Systems, vol. 63, pp. 674–680.

Ghaseminezhad, M., Doroudi, A., Hosseinian, S.H., Jalilian, A., 2017, *Analysis of Voltage Fluctuation Impact on Induction Motors by an Innovative Equivalent Circuit Considering the Speed Changes*, IET Generation, Transmission & Distribution, vol. 11(2), pp. 512–519.

Ghaseminezhad, M., Doroudi, A., Hosseinian, S.H., Jalilian, A., 2018, *Investigation of Increased Ohmic and Core Losses in Induction Motors Under Voltage Fluctuation Conditions*, Iranian Journal of Science and Technology Transactions of Electrical Engineering, vol. 43, pp. 1–10.

Ghaseminezhad, M., Doroudi, A., Hosseinian, S.H., Jalilian, A., 2021a, *Analytical Field Study on Induction Motors Under Fluctuated Voltages*, Iranian Journal of Electrical and Electronic Engineering, vol. 17(1), pp. 1620–1620.

Ghaseminezhad, M., Doroudi, A., Hosseinian, S.H., Jalilian, A., 2021b, *High Torque and Excessive Vibration on the Induction Motors Under Special Voltage Fluctuation Conditions*, COMPEL – The International Journal for Computation and Mathematics in Electrical and Electronic Engineering, vol. 40(4), pp. 822–836.

Gnaciński, P., Hallmann, D., Muc, A., Klimczak, P., Pepliński, M., 2022, *Induction Motor Supplied with Voltage Containing Symmetrical Subharmonics and Interharmonics*, Energies, vol. 15(20).

Gnaciński, P., Pepliński, M., Hallmann, D., Jankowski, P., 2019a, *The Effects of Voltage Subharmonics on Cage Induction Machine*, International Journal on Electrical Power and Energy Systems, vol. 111, pp. 125–131.

Gnaciński, P., Pepliński, M., Muc, A., Hallmann, D., Jankowski, P., 2023, *Effect of Ripple Control on Induction Motors*, Energies, vol. 16(23).

Gnacinski, P., Peplinski, M., Murawski, L., Szelezinski, A., Dec. 2019b, *Vibration of Induction Machine Supplied with Voltage Containing Subharmonics and Interharmonics*, IEEE Transactions Energy Conversion, vol. 34, pp. 1928–1937.

ISO 10816-1:1995, *Mechanical Vibration – Evaluation of Machine Vibration by Measurements on Non-Rotating Parts – Part 1: General Guidelines*.

ISO 20816-1:2016, *Mechanical Vibration – Measurement and Evaluation of Machine Vibration – Part 1: General Guidelines*.

Muttaqi, K.M., Rahman, O., Sutanto, D., Lipu, M.H., Abdolrasol, M.G., Hannan, M.A., 2022, *High-Frequency Ripple Injection Signals for the Effective Utilization of Residential EV Storage in Future Power Grids with Rooftop PV System*, IEEE Transactions on Industry Applications, vol. 58(5), pp. 6655–6665.

Nassif, A.B., 2019, *Assessing the Impact of Harmonics and Interharmonics of Top and Mudpump Variable Frequency Drives in Drilling Rigs*, IEEE Transactions on Industry Applications, vol. 55, no. 6, pp. 5574–5583.

Rahman, O., Elphick, S., Muttaqi, K.M., David, J., 2019, *Investigation of LED Lighting Performance in the Presence of Ripple Injection Load Control Signals*, IEEE Transactions on Industry Applications, vol. 55(5), pp. 5436–5444.

Ravindran, V., Busatto, T., Rönnberg, S.K., Meyer, J., Bollen, M.H.J., 2020, *Time-Varying Interharmonics in Different Types of Grid-Tied PV Inverter Systems*, IEEE Transactions on Power Delivery, vol. 35, no. 2, pp. 483–496.

Singh, R.R., Chelliah, T.R., 2017, *Enforcement of Cost-Effective Energy Conservation on a Single-Fed Asynchronous Machine Using a Novel Switching Strategy*, Energy, vol. 126, pp. 179–191.

Singh, R.R., Raj, C.T., Palka, R., Indragandhi, V., Wardach, M., Paplicki, P., 2020, *Energy Optimal Intelligent Switching Mechanism for Induction Motors with a Time Varying Load*, in IOP Conference Series: Materials Science and Engineering, Chennai, India, vol. 906, no. 1.

Tennakoon, S., Perera, S., Robinson, D., 2008, *Flicker Attenuation – Part I: Response of Three-Phase Induction Motors to Regular Voltage Fluctuations*, IEEE Transactions on Power Delivery, vol. 23(2), pp. 1207–1214.

Testa, A., Akram, M.F., Burch, R., Carpinelli, G., Chang, G., Dinavahi, V., Hatziadoniu, C., Grady, W.M., Gunther, E., Halpin, M., Lehn, P., Liu, Y., Langella, R., Lowenstein, M., Medina, A., Ortmeyer, T., Ranade, S., Ribeiro, P., Watson, N., Wikston, J., Xu, W., 2007, *Interharmonics: Theory and Modeling*, IEEE Transactions Power Delivery, vol. 22, pp. 2335–2348.

Tsiakalos, A., Tsiamitros, D., Tsiakalos, A., Stimoniaris, D., Ozdemir, A., Roumeliotis, M., Asimopoulos, N., 2021, *Development of an Innovative Grid Ancillary Service for PV Installations: Methodology, Communication Issues and Experimental Results*, Sustainable Energy Technologies and Assessments, vol. 44.

Yang, Y., Dennetière, S., 2009, *Modeling of the Behavior of Power Electronic Equipment to Grid Ripple Control Signal*, Electric Power Systems Research, vol. 79(3), pp. 443–448.